Real-time observation of electron-stimulated effects on Si(001)-(2 × 1) by optical reflectance spectroscopic methods

2007 J. Phys.: Condens. Matter 19 446008

(http://iopscience.iop.org/0953-8984/19/44/446008)

IOP Publishing Journal of Physics: Condensed Matter

J. Phys.: Condens. Matter **19** (2007) 446008 (7pp) doi:10.1088/0953-8984/19/44/446008

Real-time observation of electron-stimulated effects on Si(001)-(2 × 1) by optical reflectance spectroscopic methods

S Ohno[1,3], J Takizawa[1], J Koizumi[1], F Mitobe[1], R Tamegai[1], T Suzuki[2], K Shudo[1] and M Tanaka[1]

[1] Department of Physics, Faculty of Engineering, Yokohama National University, Tokiwadai 79-5, Hodogaya-ku, Yokohama 240-8501, Japan
[2] Department of Applied Physics, School of Applied Sciences, National Defense Academy, Hashirimizu 1-10-20, Yokosuka 239-8686, Japan

E-mail: sohno@ynu.ac.jp

Received 25 May 2007, in final form 14 August 2007
Published 24 September 2007
Online at stacks.iop.org/JPhysCM/19/446008

Abstract

We have studied the process of electron-stimulated defect formation on a Si(001)-(2 × 1) surface by means of a combination of two different surface optical methods, surface differential reflectance spectroscopy and reflectance anisotropy spectroscopy. Time courses obtained with both methods followed an exponential curve during electron irradiation over the range of 100–1000 eV. The spectral features and related physical phenomena are discussed.

1. Introduction

Low-energy electron beams under 5000 eV have been routinely used to investigate the structural and chemical properties of surfaces [1]. For example, low-energy electron diffraction (LEED) and Auger electron spectroscopy (AES) are conventional surface analysis tools used to study the crystallographic and compositional properties of surfaces with electron beams in the energy range of 20–5000 eV. There is extensive literature dealing with electron-stimulated desorption [2]. Surface reaction enhancement, typically involving oxidation processes, by low-energy electron bombardment has been observed on both semiconductor surfaces [3] and metal surfaces [4]. Electron irradiation was found to be effective for structural modification of a clean Si surface [5]. Electron-stimulated decomposition of organic molecules might be a promising means for attaching DNA to organic compounds on semiconductor surfaces [6].

Optical spectroscopies, specifically employing low-energy photons in the visible to near-ultraviolet range, are suitable means for studying electron-stimulated effects on surfaces,

[3] Author to whom any correspondence should be addressed.

0953-8984/07/446008+07$30.00

because the probe beams have quite small effects on the surface properties during measurement. In this work, we investigated electron-stimulated structural changes on Si(001) in real time by means of surface differential reflectance (SDR) spectroscopy and reflectance anisotropy spectroscopy (RAS; also known as reflectance difference spectroscopy, RDS). Among the available optical methods, SDR allows the measurement of different chemical reactions at various adsorption sites, separately and simultaneously, while RAS is sensitive to change of surface anisotropy. Both techniques are applicable in various environments, from ultrahigh-vacuum conditions to catalytic and corrosive conditions at high pressure and at a solid/liquid interface [7].

High-energy electron beam irradiation at 20 keV is used to fabricate silicon nanoislands [8]. In contrast, the use of low-energy electrons may have potential for atomic level control of tailored nanostructures, because the relevant excitation process is localized at a specific site [5]. In this study, we report the real-time observation of possible defect formation processes on a Si(001)-(2 × 1) surface. Although the physical origins of the spectral features are not yet well understood, our results demonstrate that SDR and RAS are useful for the characterization of electron-stimulated effects on silicon surfaces.

2. Experimental details

Experiments were performed with an ultrahigh-vacuum chamber, whose base pressure was under 2.0×10^{-8} Pa. The sample used was a p-type Si(001) single crystal with resistivity of 12.0–14.0 Ω cm, cut to the size of $3 \times 20 \times 0.63$ mm^3. We used a Si(001) wafer with a miscut at 4° towards the [110] direction to acquire single-domain Si(001)-(2 × 1) structure. Heating was performed by applying direct current to the sample. The sample was well degassed for over 12 h at 873 K and cleaned by flashing at 1470 K for 10 s. It was then subjected to electron irradiation at room temperature.

The optical set-up of SDR has been described elsewhere [9]. A xenon lamp was used as the light source from the visible to near-ultraviolet region (1.5–6.0 eV). The p-polarized light was applied to the surface with an incident angle of about the Brewster angle, at which reflectance from the substrate is considered to be minimized [10]. The SDR intensity is defined as

$$\frac{\Delta R}{R} = \frac{R_\mathrm{a} - R_\mathrm{c}}{R_\mathrm{c}} \tag{1}$$

where R_c and R_a represent the reflectances of the clean surface and that of the reacted surface, respectively.

The optical set-up for the RA measurements was designed following the configuration reported by Aspnes *et al* [11]. We used a strain-free window to minimize optical anisotropy irrelevant to the surface structure. A xenon lamp was used as the light source. The incident light polarized in the [010] direction was introduced almost normal to the surface. Reflected light was monochromated with a monochromator located in front of the photomultiplier. The RA amplitude, $\Delta r/r$, is defined as

$$\frac{\Delta r}{r} = \frac{2(r_a - r_b)}{r_a + r_b} \tag{2}$$

where r_a and r_b are complex reflectances for polarization parallel and perpendicular to the direction of the dimer bonds on a clean Si(001)-(2 × 1) surface, respectively. The real part of the RA amplitude ($\Delta R/R = \mathrm{Re}(\Delta r/r)$) was exclusively analyzed, since the real part and the imaginary part are connected via the Kramers–Kronig relation.

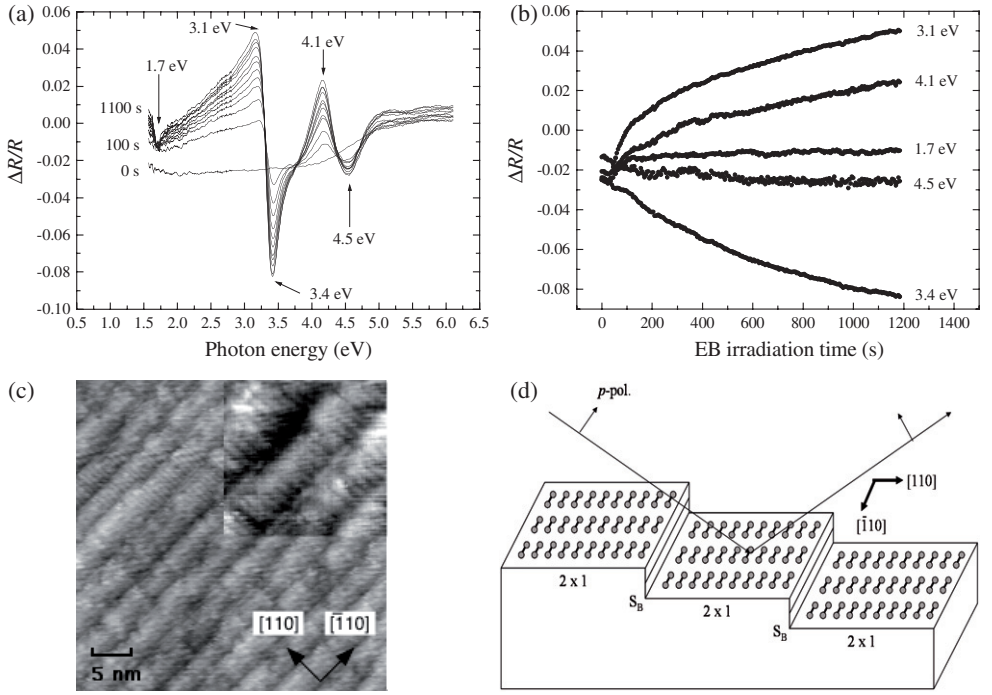

Figure 1. (a) A series of SDR spectra obtained during 1 keV electron irradiation of a Si(001)-(2 × 1) surface. The flux of 6.0×10^{11} electrons mm^{-2} corresponds to ∼0.2 electrons per dimer. (b) Time courses of SDR intensity at different photon energies. (c) Empty state STM image of a Si(001)-(2 × 1) surface with 4° miscut. The tunneling current was 0.1 nA and the sample bias was +2.0 V. (d) Schematic of a single-domain Si(001)-(2 × 1) surface separated by a double step perpendicular to the dimer row, as denoted by S_B.

3. Results and discussion

Figure 1(a) shows SDR spectra obtained during irradiation with 6.0×10^{11} electrons mm^{-2} s^{-1} at 1000 eV on a Si(001)-(2 × 1) surface. Two positive peaks can be seen at 3.1 and 4.1 eV and two negative peaks at 3.4 and 4.5 eV. These negative peaks are related to the electronic states relevant to bulk critical point energies of E_1 (3.5 eV) and E_2 (4.3 eV) transitions. The uptake curves at several photon energies are depicted in figure 1(b). In a separate chamber, we confirmed with scanning tunneling microscopy (STM) that single-domain Si(001)-(2 × 1) structure is formed using the same preparation method, as shown in figure 1(c). The quality of the surface structure was also checked using LEED. The p-polarized light is incident along the [110] direction perpendicularly to the dimers, as schematized in figure 1(d).

To our knowledge, there are no reports on theoretical calculations of optical reflectance spectra associated with defect formation on Si(001)-(2 × 1). Therefore, we compared our results with a benchmark system of hydrogen adsorption on the same surface. The evolution of SDR spectra with time during the hydrogen adsorption process on a Si(001)-(2 × 1) surface is shown in figure 2. When hydrogen is adsorbed at room temperature, the surface forms a poorly ordered dihydride Si(001)-(1 × 1):H structure. At high temperature of 573 K, a perfect monohydride Si(001)-(2 × 1):H structure is formed [12]. It is possible to distinguish the two structures with p-polarized light, as shown in figure 2. Energies of negative peaks are slightly redshifted for the spectra at 573 K, and the valley structure between them at around 3.5 eV

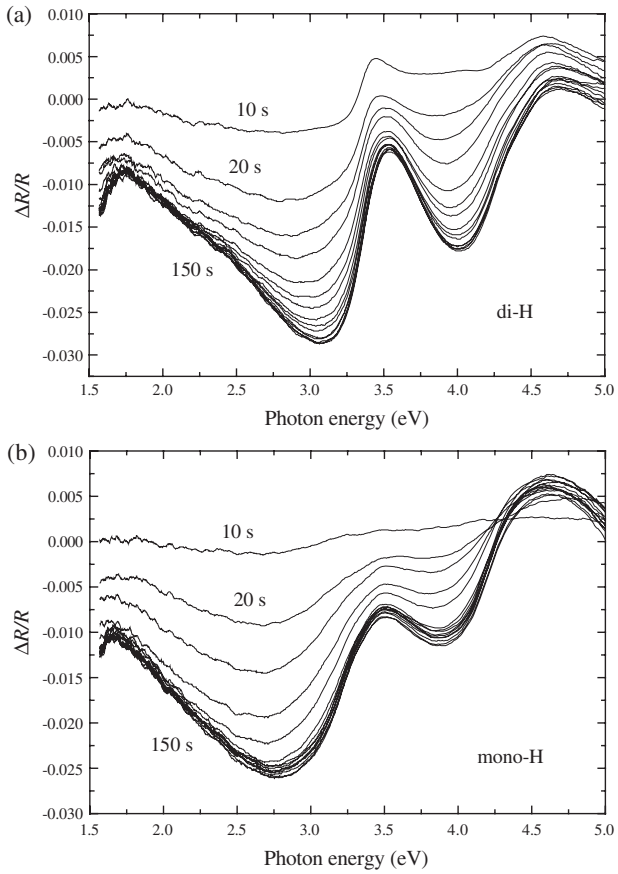

Figure 2. SDR spectra taken during exposure of atomic hydrogen upon a Si(001)-(2 × 1) surface. Atomic hydrogen was produced with a hot tungsten filament at 2.4 A under a hydrogen pressure of 1.0×10^{-3} Pa (a) at room temperature and (b) at 573 K.

is shallower for monohydride formation. Such features are also recognizable with s-polarized light in a similar optical set-up, although the SDR signal appears to be smaller [13]. It should be noted that the spectral intensity may change slightly with optical configuration for s-polarized light [14].

In the case of electron irradiation, the prominent positive peaks and the valley structure have opposite signs compared with those for a hydrogen adsorbed surface. The spectral features appear to be analogous to those obtained with modulation spectroscopies, such as electroreflectance or piezoreflectance [15]. These methods have been extensively used to investigate bulk properties of band structures in semiconductors. The present SDR spectra appear similar to differential-type spectra due to the rigid shift of the bulk dielectric function. We consider that SDR features are due to the surface-modified bulk transitions, as often discussed in the interpretation of RAS features [16]. The reflectance signal derived from the change of bulk dielectric function obtained by the conventional modulation spectroscopy is usually at the order of 10^{-4}–10^{-5}. In contrast, the reflectance signal is much larger with SDR, being of the order of 10^{-2}. Thus, the present results suggest that the local lattice strain caused by the defect formation near the surface may produce much larger modulation in the dielectric function.

The SDR spectral features presumably originate from modification of structures on the Si(001)-(2 × 1) surface, although details of the electronic structures are unknown. In the case of hydrogen adsorption, the dimer bond can be broken for dihydride formation. Only negative signals are observed for the hydrogenation process, as in the case of oxidation and halogen adsorption processes [17, 18]. In these cases, we have confirmed that the SDR signals are almost proportional to the coverage of adsorbates, and the adsorption sites can be resolved, as confirmed with STM [19]. As the reflectance from the hydrogen adsorbed surface is similar to that from the bulk silicon, the double-peak structures in figure 2 are ascribed to optical response related to the intrinsic surface states [13]. The large difference of the spectral features for the defect formation in figure 1 suggests that production of dimer vacancies largely affects the Si dielectric function at the surface or even at subsurface regions.

In the early STM work, the density of dimer vacancies and agglomerated vacancy complexes increased almost linearly with electron irradiation time at 2000 eV, at vacancy coverage below 0.25 ML [5]. In the present SDR measurements, prolonged electron irradiation resulted in exponential uptake curves at several peak energies, as shown in figure 1(b). The intensity of the SDR signal may be proportional to the density of vacancies, as suggested in the reaction with gas molecules or activated atoms [13, 17–19]. The SDR intensity obtained by electron irradiation turned out to be much larger than that obtained by hydrogen adsorption. This may suggest that the electron beam produces vacancies and subsequent lattice strain even at subsurface regions not accessible with STM.

We further investigated the formation kinetics of defects on Si(001)-(2 × 1) by means of RAS. Compared with SDR, RAS is rather sensitive to the anisotropy at surface layers. In figure 3(a), we show the RA spectrum for a clean surface and that obtained after electron irradiation. The spectral features of the clean Si(001)-(2 × 1) are consistent with the literature [20]. A typical RA time course at 3.1 eV is depicted in figure 3(b). At the flux of 8.9×10^{10} electrons mm^{-2} s^{-1} at 1000 eV, we observed a steep increase of RA intensity at the initial stage and a gradual increase towards saturation, as seen with SDR. In figure 3(c), we show the time course in the case of 100 eV electron irradiation at the flux of 8.9×10^{10} electrons mm^{-2} s^{-1}. No qualitative difference in the spectral features other than the reaction rate was observed up to 100 eV. Hence, the mechanism of defect formation remains qualitatively the same in the energy range of 100–1000 eV.

At the photon energy of 3.1 eV near the E_1 critical point, the RA signal changes from negative to positive during electron irradiation. This feature is similar to the oxidation process in the layer-by-layer mode with a smooth interface [21]. For initial oxidation in a monolayer regime, the origin of the RA signal around 3.1 eV can be ascribed to the deformation of the silicon lattice induced by oxidation, rather than to the oxygen-derived electronic states, during the formation of an oxide island [22]. There are several oxygen adsorption sites, leading to structural complexity of the oxide islands. However, it is possible that the origin of the RA signal during electron irradiation can be ascribed to the Si lattice strain produced by the defect formation. A small peak structure around 3.1 eV appears after oxygen exposure of 200 L at room temperature [16]. The structureless feature is similar to the present data for electron irradiation, compared with the interaction with hydrogen, water or other organic molecules [16]. Considering this similarity, it should be noted that formation of a dimer vacancy may also take place in the oxidation process. Recent first-principles calculations showed that a single dimer vacancy is preferentially formed after oxygen adsorption at low coverage [23]. An early STM study showed that this dimer ejection process involving oxygen can be thermally activated by annealing up to 570 K [24]. The RA spectral features due to the dimer ejection process could be investigated with RAS to clarify the role of mobile Si species on the surface during oxidation, which may be analogous to electron-stimulated defect formation.

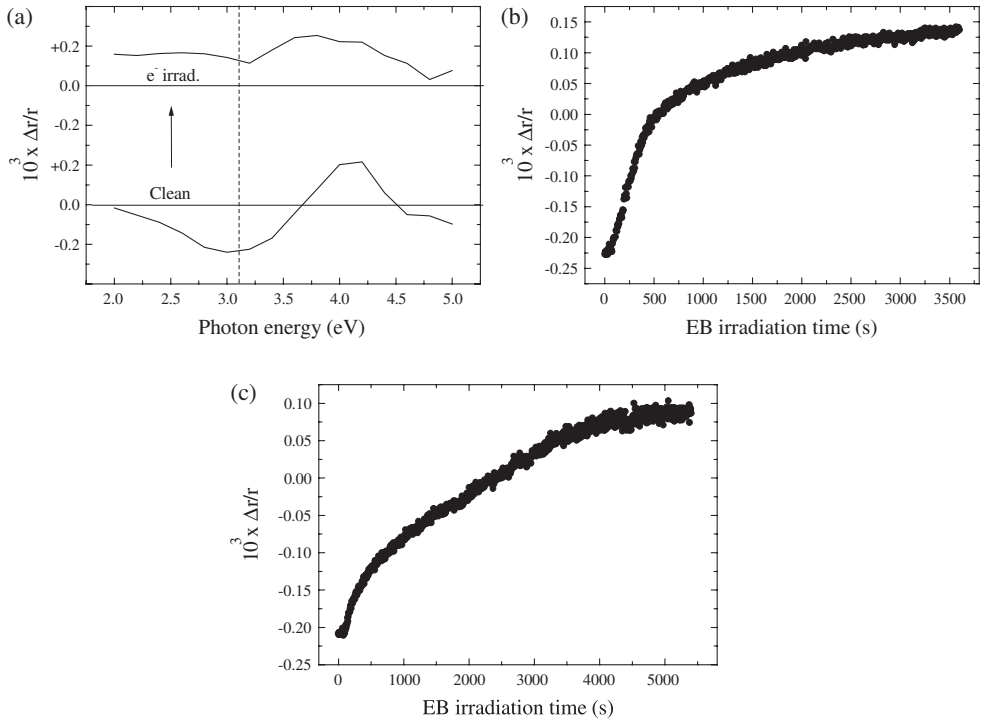

Figure 3. (a) RA spectra of a clean Si(001)-(2 × 1) surface and the surface after 1 keV electron irradiation for 1 h. (b) Time course of RA intensity at 3.1 eV during 1 keV electron irradiation for 1 h. The flux of 8.9×10^{10} electrons mm^{-2} corresponds to ∼0.03 electrons per dimer. (c) Time course of RA intensity at 3.1 eV during 100 eV electron irradiation for 1.5 h. The flux is the same as in (b).

Our present results suggest that electron beams of 100–1000 eV predominantly produce vacancies on Si(001)-(2 × 1). On the other hand, electron irradiation below 50 eV on Si(001)-(2 × 1) may cause qualitatively different phenomena. For example, an STM study showed that subsurface damage produced by Ar^+ ion bombardment was reversed by 25 eV electron irradiation [25]. A low-temperature LEED study at 24 K revealed a partial structural change from c(4 × 2) to p(2 × 2) structure upon electron beam irradiation at 50 eV on a timescale of less than a minute [26]. Our results indicate that it will be possible to detect and further analyze these subtle effects by the use of surface optical spectroscopic techniques.

4. Conclusion

We have observed electron-stimulated effects on a Si(001)-(2 × 1) surface by means of SDR and RAS. Spectral features around the E_1 and E_2 critical points were identified with both methods. The spectral time courses exhibited similar exponential-like uptake curves. We suggest that these observations can be ascribed to the vacancy formation produced by electron irradiation on this surface.

Acknowledgments

We would like to thank Dr T Yasuda of the National Institute of Advanced Industrial Science and Technology (AIST) for valuable help in constructing the RAS apparatus. This

work was supported in part by a Grant-in-Aid for Scientific Research, as well as funds from the Foundation for Promotion of Material Science and Technology of Japan (MST Foundation), Iketani Science and Technology Foundation, Yokohama Kogyokai Foundation, Yokohama Academic Foundation, and Nippon Sheet Glass Foundation for Materials Science and Engineering.

References

[1] Woodruff D P and Delchar T A 1986 *Modern Techniques of Surface Science* (Cambridge: Cambridge University Press)
[2] Ramsier R D and Yates J T Jr 1991 *Surf. Sci. Rep.* **12** 243
[3] Ohno S and Yates J T Jr 2005 *J. Vac. Sci. Technol.* A **23** 475
Xu J, Choyke W J and Yates J T Jr 1997 *J. Appl. Phys.* **82** 6289
[4] Zhukov V, Popova I and Yates J T Jr 2002 *Phys. Rev. Lett.* **89** 276101
[5] Nakayama K and Weaver J H 1999 *Phys. Rev. Lett.* **82** 980
[6] Lozano J, Early D, Craig J H Jr, Wang P W and Kimberlin K R 2005 *Surf. Interface Anal.* **37** 366
[7] Weightman P, Martin D S, Cole R J and Farrell T 2005 *Rep. Prog. Phys.* **68** 1251
McGilp J F 1995 *Prog. Surf. Sci.* **49** 1
[8] Johnson S, Markwitz A, Rudolphi M and Baumann H 2004 *J. Appl. Phys.* **96** 605
[9] Tanaka M, Shirao T, Sasaki T, Shudo K, Washio H and Kaneko N 2002 *J. Vac. Sci. Technol.* A **20** 1358
[10] Horikoshi Y, Kawashima M and Kobayashi N 1991 *J. Crystal Growth* **111** 200
[11] Aspnes D E, Harbison J P, Studna A A and Florez L T 1988 *J. Vac. Sci. Technol.* A **6** 1327
[12] Boland J J 1993 *Adv. Phys.* **42** 129
[13] Borensztein Y, Pluchery O and Witkowski N 2005 *Phys. Rev. Lett.* **95** 117402
[14] Borensztein Y and Witkowski N 2004 *J. Phys.: Condens. Matter* **16** S4301
[15] Lautenschlager P, Garriga M, Viña L and Cardona M 1987 *Phys. Rev.* B **36** 4821 and references therein
[16] Witkowski N, Coustel R, Pluchery O and Borensztein Y 2006 *Surf. Sci.* **600** 5142
[17] Tanaka M, Yamakawa E, Shirao T and Shudo K 2003 *Phys. Rev.* B **68** 165411
Tanaka M, Minami S, Shudo K and Yamakawa E 2003 *Surf. Sci.* **527** 21
[18] Takizawa J, Ohno S, Koizumi J, Shudo K and Tanaka M 2006 *J. Phys.: Condens. Matter* **18** L209
[19] Owa Y, Shudo K, Koma M, Iida T, Ohno S and Tanaka M 2006 *J. Phys.: Condens. Matter* **18** 5895
[20] Yasuda T, Nishizawa M, Kumagai N, Yamasaki S, Oheda H and Yamabe K 2004 *Thin Solid Films* **455/456** 759
[21] Yasuda T, Kumagai N, Nishizawa M, Yamasaki S, Oheda H and Yamabe K 2003 *Phys. Rev.* B **67** 195338
[22] Fuchs F, Schmidt W G and Bechstedt F 2005 *Phys. Rev.* B **72** 075353
[23] Yu B D, Kim Y J, Jeon J, Kim H, Yeom H W, Lyo I W, Kong K-J, Miyamoto Y, Sugino O and Ohno T 2004 *Phys. Rev.* B **70** 033307
[24] Avouris Ph and Cahill D 1992 *Ultramicroscopy* **42–44** 838
[25] Narushima T, Kitajima M and Miki K 2004 *J. Phys.: Condens. Matter* **16** L193
[26] Mizuno S, Shirawasa T, Shiraishi Y and Tochihara H 2004 *Phys. Rev.* B **69** 241306